



Minerva Access is the Institutional Repository of The University of Melbourne

Author/s:

Chen, GQ;Gras, SL;Kentish, SE

Title:

Eutectic freeze crystallization of saline dairy effluent

Date:

2020-04-15

Citation:

Chen, G. Q., Gras, S. L. & Kentish, S. E. (2020). Eutectic freeze crystallization of saline dairy effluent. *Desalination*, 480, <https://doi.org/10.1016/j.desal.2020.114349>.

Persistent Link:

<https://hdl.handle.net/11343/237423>

Eutectic Freeze Crystallization of Saline Dairy Effluent

G. Q. Chen¹, S. L. Gras^{1,2}, S. E. Kentish^{1*}

¹ The ARC Dairy Innovation Hub, Department of Chemical Engineering, University of Melbourne, Victoria 3010, Australia.

² The Bio21 Molecular Science and Biotechnology Institute, The University of Melbourne, Parkville, Victoria 3010, Australia

Keywords: Dairy; whey; Eutectic temperature; Phase diagram; Sodium chloride.

*Corresponding Author

Prof S. Kentish

Tel: +61 3 8344 6682

Fax: +61 3 8344 4153

E-mail address: sandraek@unimelb.edu.au

1 **ABSTRACT**

2

3 The disposal of saline effluent in the dairy industry is subject to increasingly strict regulatory requirements. In
4 this work, eutectic freeze crystallization (EFC) was investigated as a mechanism for the simultaneous separation
5 of salts and ice in a typical saline effluent, namely salty whey. Experiments were conducted using salty whey
6 samples collected from a dairy processing facility. The eutectic point of the salty whey was determined using
7 differential scanning calorimetry and was found to be lower than that of NaCl solutions (-24°C for salty whey vs.
8 -21°C for aqueous NaCl solutions). Crystallization experiments were then used to construct the phase diagram
9 of this dairy stream under equilibrium conditions. The change in cation composition in the supernatant at the
10 eutectic temperature was measured as a function of time and showed that pure NaCl salts and ice formed within
11 five minutes after this temperature was reached. The energy consumption of this process was estimated to be
12 ~ 120 kWh/tonne for salty whey, which is comparable to that for conventional thermal crystallization of brine.

14 1. INTRODUCTION

15

16 Salt is a key component within dairy manufacturing, both as a result of the natural mineral levels in
17 milk but also as sodium chloride directly added during cheese making [1]. For example, sodium
18 chloride is added to the cheese curd to lower the water activity within the curd, when making semi-
19 hard or hard cheeses such as Cheddar or Colby. Only about 35-50% of the added salt is retained in the
20 curd. The excessive moisture is expelled from the curd during salting and pressing processes, together
21 with a significant amount of the added salt, forming salty whey. Salty whey is one of several effluent
22 streams generated by the dairy industry that is subject to increasingly strict regulatory requirements
23 for disposal, due to the increase in agricultural water usage and local land degradation caused by
24 sodium leaching. Thermal evaporation and membrane processes are commonly employed to reduce
25 the volume of these effluent streams and to improve their quality before discharge [2].

26 Salty effluents are of low economic value and so any separation process should be performed at
27 minimum cost. The saturation concentration of NaCl in water is 35 wt% at ambient temperature and
28 varies little as this temperature changes [3]. This means that a large amount of water must be removed
29 for evaporative crystallization from these effluents to occur, making this a costly approach. Freeze
30 concentration processes have been developed as an alternative in the food and beverage
31 manufacturing industry [4-6] as well as in the desalination industry [7, 8], to remove water in the form
32 of ice. Such an approach can be more energetically favourable as the enthalpy of freezing is much
33 lower than the enthalpy of evaporation (e.g., $\Delta H_{\text{fus}} = 334 \text{ J/g}$ and $\Delta H_{\text{vap}} = 2265 \text{ J/g}$ for water). In
34 particular, eutectic freeze concentration (EFC) is an emerging technology that operates at the eutectic
35 temperature of the solution to enable simultaneous separation of saline solutions into ice and salt [9],
36 with advantages of energy reduction, high salt purity and an absence of additional chemicals [10]. EFC
37 can overcome the limited temperature sensitivity of sodium chloride to crystallization and the high
38 energy demand of evaporation, by reaching saturation at a lower concentration (23.3 wt%) at the
39 eutectic temperature.

40 A typical phase diagram for a salt-water system is shown in Figure 1. When an unsaturated solution is
41 cooled from point A to the temperature corresponding to its concentration on the ice line, ice begins
42 to form in the now saturated solution. A further decrease in temperature causes the system to become
43 more concentrated due to the crystallization of ice and to eventually reach the eutectic point, the
44 lowest possible temperature of crystallization. At this point, crystalline salt structures and ice crystals
45 form separately and can be separated due to the large density difference between ice (0.92 g/cm^3)
46 and salts (e.g NaCl 2.17 g/cm^3). In a batch process, this can be observed when stirring is turned off [9].
47 In a continuous process, two extra separators are required, one to process the ice slurry and wash the

48 ice with recycled pure water, and another to wash the salt with a saturated solution [11, 12].

49

50

51

52

53

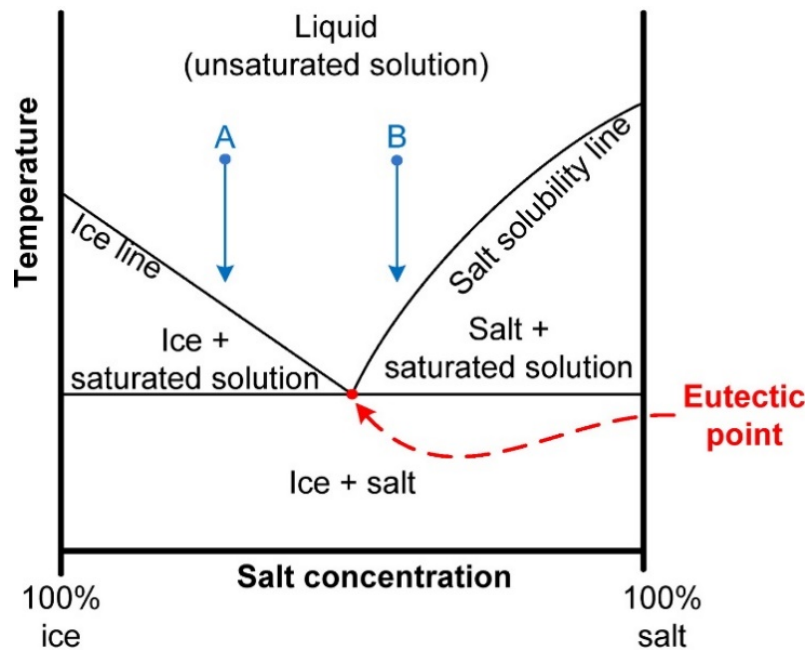
54

55

56

57

58



59 Figure 1: A typical phase diagram for aqueous salt solutions showing the Eutectic point [13]. (Copyright
60 2012, with permission from Elsevier.)

61

62 A life cycle assessment comparing EFC and evaporative crystallization indicated that EFC processes
63 have great potential to reduce the energy consumption and carbon footprint of the crystallization
64 units [14]. It was found that the EFC process consumes 6-7 times less energy when compared to
65 evaporative crystallization for a 4 wt% model solution of sodium sulphate [14]. Van der Ham et al. [9]
66 found that EFC could reduce the energy required to recover sodium nitrate (from 35 wt% aqueous
67 solution) and copper sulphate (from 12 wt% aqueous solution) by 30% and 65%, respectively,
68 compared to multi-step evaporation. Randall et al. [15] also demonstrated that EFC could convert 97%
69 of the liquid to pure water, calcium sulphate (98.0% purity) and sodium sulphate (96.4% purity), when
70 processing the brine stream generated by a reverse osmosis process (i.e., reverse osmosis
71 concentrate) from the mining industry. EFC has been commercialised by a number of companies
72 internationally. Cool Separations (The Netherlands) have developed single stage EFC that can handle
73 multi-component systems and multi-stage EFC that can crystallise out the specific salts in sequence
74 by operating a series of crystallisers at different temperatures. Other companies include Eskom (South
75 Africa), PROXA Water (South Africa) and Prentec Pty Ltd (South Africa).

76 Salty whey from cheese manufacturing plants comprises a high concentrations of sodium chloride (50-
77 70 wt% of the total solids [16]), with a small amount of organic matter such as milk sugar and organic

78 acids, as well as divalent salts such as calcium phosphate (2.5-5 wt% of total solids [16]). The
79 composition of the fresh salty whey sample collected in this study is shown in Table 1.

80 In Australia, salty whey is typically managed in evaporation lagoons where water is naturally
81 evaporated. However, the construction of further evaporation ponds in some areas is now banned
82 due to environmental impacts from land degradation, odour and dust [2]. In this work, eutectic freeze
83 crystallization of salts and ice from fresh salty whey samples collected from a dairy factory is carried
84 out using a well-insulated crystallization reactor. The fresh salty whey samples are also allowed to
85 evaporate naturally to achieve a concentration factor of 2, mimicking the brine present in the
86 evaporation lagoons. The phase diagram, composition of supernatant and salts, as well as the energy
87 demand for processing fresh salty whey and concentrated salty whey samples are investigated. To the
88 best of our knowledge, this is the first study performed to demonstrate the applicability of EFC
89 technology in processing saline effluent from the dairy industry.

90

91 **2. EXPERIMENTAL**

92 **2.1 Materials**

93 Solutions of different concentrations of sodium chloride (99.7%, AR Grade, Chem-supply Australia)
94 were prepared in the laboratory for method validation. Salty whey samples were collected from a
95 dairy processing facility in Victoria, Australia, after ultrafiltration (UF) was used to recover the protein.
96 These samples are therefore referred to as salty whey (UF permeate). The composition of the salty
97 whey (UF permeate) was typical of that commonly found in a dairy processing facility [16]. Some salty
98 whey samples (UF permeate) obtained from a dairy company were naturally evaporated at room
99 temperature to double the total solids content, mimicking evaporation in an evaporation pond. The
100 pH of these concentrated samples decreased by 1 pH unit, due to the conversion of some lactose by
101 lactic acid bacteria, as would also occur naturally in an evaporation pond. The decrease in pH caused
102 some residual proteins to precipitate. The concentrated salty whey samples were thus filtered using
103 a 0.22 μm Polyethersulfone (PES) filter before being processed in the crystalliser. This is referred to as
104 evaporated and filtered (E&F) salty whey. The E&F salty whey was also diluted from 30% to 16% to
105 study the effect of partial organic removal using the PES filter. Table 1 below shows the composition
106 of the raw, concentrated and diluted salty whey samples.

107

108

109 Table 1: General characteristics and composition of salty whey (UF permeate), evaporated and
 110 filtered salty whey (E&F Salty Whey) and diluted E&F salty whey (Dil-E&F Salty Whey).

Description	Unit	Salty Whey (UF Permeate)	Evaporated & Filtered* Salty Whey (E&F Salty Whey)	Diluted# E&F Salty Whey (Dil-E&F Salty Whey)
Conductivity	mS/cm	132 ± 3	171 ± 3	137 ± 3
pH	-	5.13 ± 0.04	3.94 ± 0.03	ND
Total Solids	%	14.7 ± 0.1	30.2 ± 0.2	16.0 ± 0.1
Ash	%	10.8 ± 0.7	19.9 ± 1.3	10.6 ± 0.7
Organic Matter	%	3.9 ± 0.6	10.3 ± 1.5	5.4 ± 0.8
Na	g/L	41.4 ± 1.2	77.7 ± 2.3	44.3 ± 1.3
K	g/L	1.39 ± 0.05	3.21 ± 0.13	1.64 ± 0.06
Mg	g/L	0.14 ± 0.01	0.29 ± 0.01	0.14 ± 0.01
Ca	g/L	1.52 ± 0.05	2.43 ± 0.08	1.17 ± 0.04
P [^]	g/L	0.74 ± 0.03	1.23 ± 0.05	0.99 ± 0.04

* Prepared by evaporation of salty whey (UF Permeate) at 30 ± 5 °C followed by filtration with by 0.22-micron PES (Polyethersulfone) filters

Dilution factor: 2

[^] Phosphorus (P) is present as phosphate ions. *Chloride ions (not determined) are the primary anions in the sample with a similar molar concentration to that of sodium [16].*

ND: Not determined

111

112 2.2 EFC Reactor

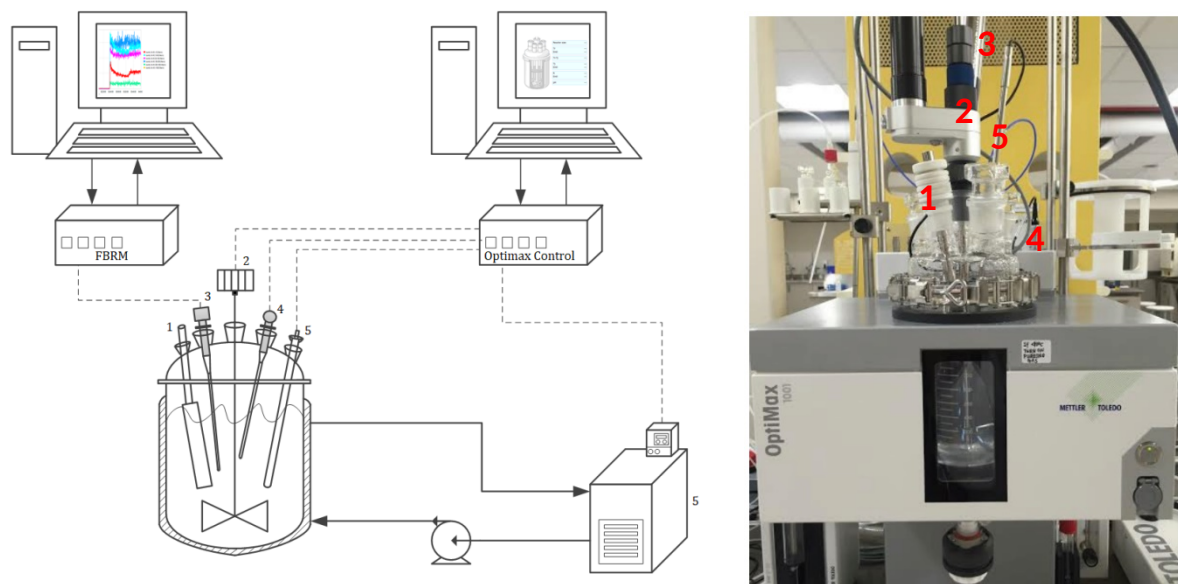
113 A crystallization reactor of 1 L (Optimax 1001 Mettler Toledo) was used to study the freezing process
 114 (Figure 2). The reactor can be operated from -30 °C to 180 °C, using a reactor jacket with an ethylene
 115 glycol and water mixture as the circulated cooling medium. The temperature was recorded using a
 116 temperature probe, while a calorimetric probe (OptiMax™ HFCal) was used to measure the heat flow
 117 between the reactor and the jacket. A focused beam reflectance measurement (FBRM) sensor was
 118 used to collect estimates of the particle size within a range ranging from <10 μm to ~1000 μm. It should
 119 be noted that rather than a particle diameter, the FBRM measures a chord length, which is defined as
 120 the distance between the two edges of a particle through which the beam passes [17]. Heat flow
 121 calorimetric information was used to estimate the specific heat capacity of the sample, which was
 122 performed by the built in program within the iControl™ Software.

123 Reactor volumes of 600 – 900 mL were used for each experiment. The reactor temperature was
 124 lowered to the desired temperature at a rate of <0.15 K/min. An overhead stirrer was used to agitate
 125 the samples within the reactor. For temperatures greater than -18 °C, a stirring speed of 300 rpm was
 126 used, while 800 – 1000 rpm was used for lower temperatures to ensure adequate mixing of the

127 solution-crystal mixture.

128 Two different approaches were used to construct the phase diagram of both the NaCl-H₂O system and
129 the salty whey system. In the first approach, the temperature of solutions of different concentration
130 was lowered until crystallization occurred, while the reactor and jacket temperatures and the
131 corresponding particle size counts were monitored. The crystallization temperature was determined
132 from a rapid change in the jacket temperature as the latent heat is dissipated from the system when
133 crystallization occurs. This was confirmed by a sharp increase in the chord length counts detected by
134 the FBRM at this temperature (see Section 3.2). The crystallization temperature was then plotted
135 against the initial total solids concentrations to form the phase diagram.

136 In the second approach, solutions of a specific concentration were cooled in a stepwise manner, with
137 samples of the supernatant taken within 5 minutes of a specific reactor temperature being reached.
138 At each temperature, the stirrer was paused for 30 seconds to allow ice crystals to float to the top
139 and/or salt crystals to settle in the reactor, so that a clear supernatant could be obtained from the
140 middle section of the reactor. Once the reactor had reached the estimated eutectic temperature (-
141 21 °C for NaCl solutions and -24 °C for salty whey) it was held at this temperature for 60 minutes
142 before a final supernatant sample was collected. The total dissolved solids concentration in the
143 supernatant was determined and was used to construct the phase diagram.



144 1 - Baffle blade, 2 - Impeller, 3 - FBRM, 4, HFCal, 5 - Temperature sensor, 6 - Water bath

145 Figure 2: The schematic of OptiMax 1001 crystalliser equipped with temperature, heat flow and FBRM
146 sensors (left); and a photo of the crystalliser without showing the water bath and computers (b).

147
148

149 **2.3 Analysis**

150 Differential Scanning Calorimetry (DSC 8500, PerkinElmer) was used to determine the eutectic
151 temperature. The samples were sealed in aluminum pans, while an empty pan was used as reference.
152 The samples were held at 25 °C for 5 minutes to stabilise the initial heat flow. A temperature scan
153 from 25 °C to -80 °C was then conducted using a linear scanning rate of 3 K/min, after which the
154 samples were heated to 25 °C at the same scanning rate.

155 Total dissolved solids and total ash were determined as per Australian Standards AS 2003.1.1 and AS
156 2003.1.5. The aqueous phase samples were weighed before drying at 110 °C overnight in an oven to
157 evaporate all moisture. The total dissolved solids was determined from this mass balance. After
158 weighing, the dried samples were further charred in a furnace at 650°C for more than 12 hours until
159 samples turned white. Organic matter was calculated as the difference between the total dissolved
160 solids and total ash content. In pure sodium chloride solutions, the total dissolved solids concentration
161 refers to the concentration of sodium chloride. In salty whey solutions, the total dissolved solids
162 include the organic matter and the total salts (ash) in the system, inclusive of sodium chloride and
163 other salts such as calcium phosphate. Further, Inductively Coupled Plasma Atomic Emission
164 Spectroscopy (ICP-OES 720ES, Varian) was used to determine the concentrations of sodium, potassium,
165 calcium, magnesium and phosphorus within the ash.

166

167 **3. RESULTS AND DISCUSSION**

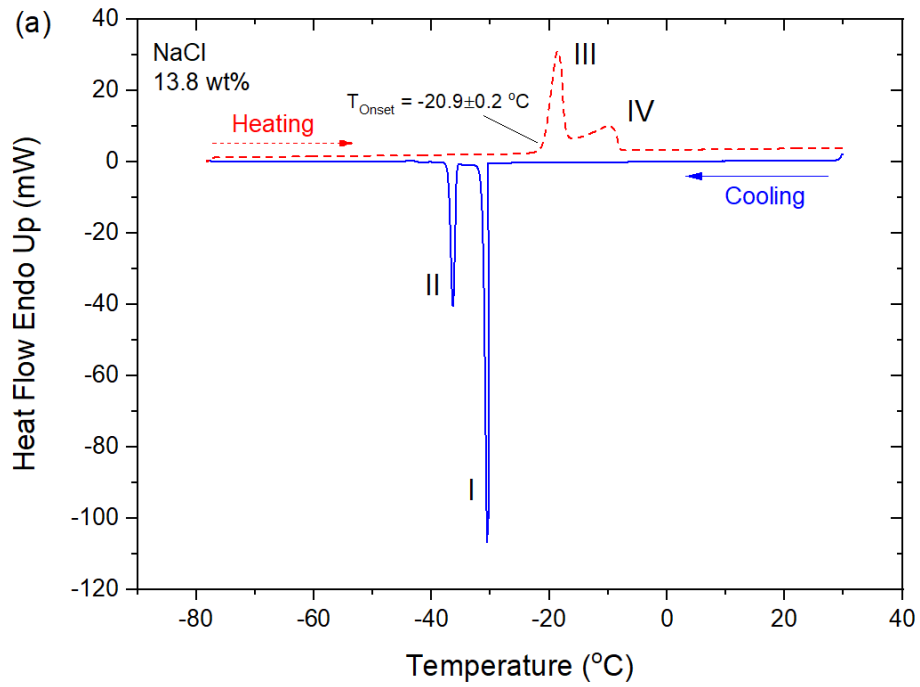
168 **3.1 Eutectic Temperature**

169 DSC thermograms were used to determine the eutectic temperature. The technique was initially used
170 with pure sodium chloride to validate the method and determine its precision. Figure 3 (a) shows the
171 DSC thermograms of a 13.8% NaCl solution, which is indeed consistent with the literature [18, 19].
172 The first transition temperature T(I) on the cooling curve is the temperature at which ice crystals
173 appear in the solution. T(II) represents the non-equilibrium crystallization of NaCl from a super-
174 saturated solution, which is much lower than the equilibrium eutectic temperature (i.e. -36°C versus
175 -21 °C). This is typical behavior observed during cooling of NaCl solutions[18]. During heating, the
176 transition temperature T(III) represents the true eutectic temperature of NaCl (-20.9 ± 0.2°C) as these
177 crystals melt, while transition IV is caused by the melting of ice in the sample at ~0°C.

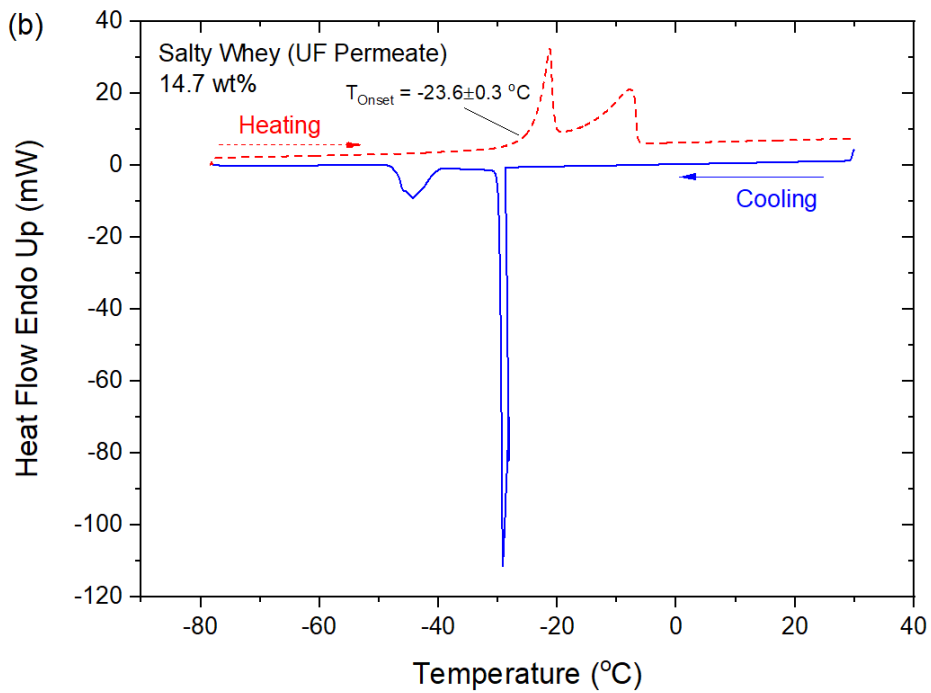
178

179 Given salty whey contains mostly sodium chloride, the eutectic freeze temperature of salty whey is
180 expected to be similar to a NaCl-H₂O system. Samples of salty whey (UF permeate) and evaporated &

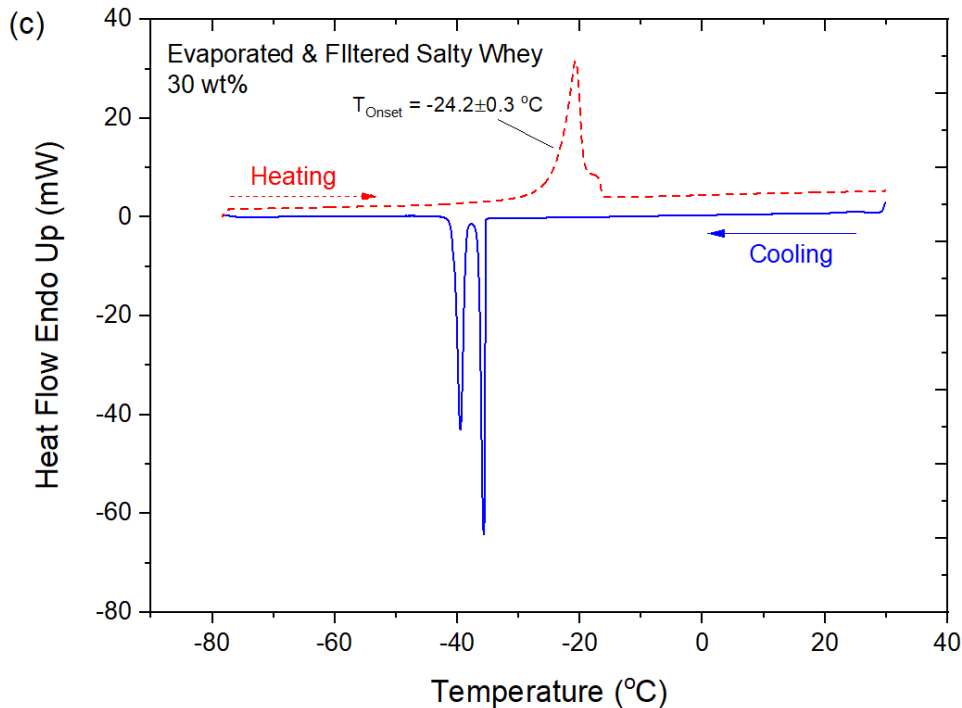
181 filtered salty whey were also scanned by the DSC to produce similar thermograms (Figures 3(b) and
182 (c)). It can be seen that both samples show similar heat flow curves during heating and cooling, with
183 the eutectic point of the salty whey samples collected for this study being $-23.6 \pm 0.3 \text{ }^\circ\text{C}$ for salty whey
184 (UF permeate) and $-24.2 \pm 0.3 \text{ }^\circ\text{C}$ for evaporated & filtered salty whey.
185



186



187



188

189 Figure 3: DSC thermograms (heat flow vs. temperature) measured during cooling (I and II) from 30°C
 190 to -80 °C and subsequent heating (III and IV) for (a) 13.8% NaCl in water, (b) salty whey (UF permeate)
 191 and (c) evaporated & filtered salty whey. The scanning rate was 3°C/min for both cooling and heating
 192 steps. The eutectic temperatures were determined to be $-20.9 \pm 0.2 \text{ } ^\circ\text{C}$, $-23.6 \pm 0.3 \text{ } ^\circ\text{C}$, and $-24.2 \pm$
 193 $0.3 \text{ } ^\circ\text{C}$ for 13.8% NaCl in water, salty whey (UF permeate) and evaporated & filtered salty whey,
 194 respectively.

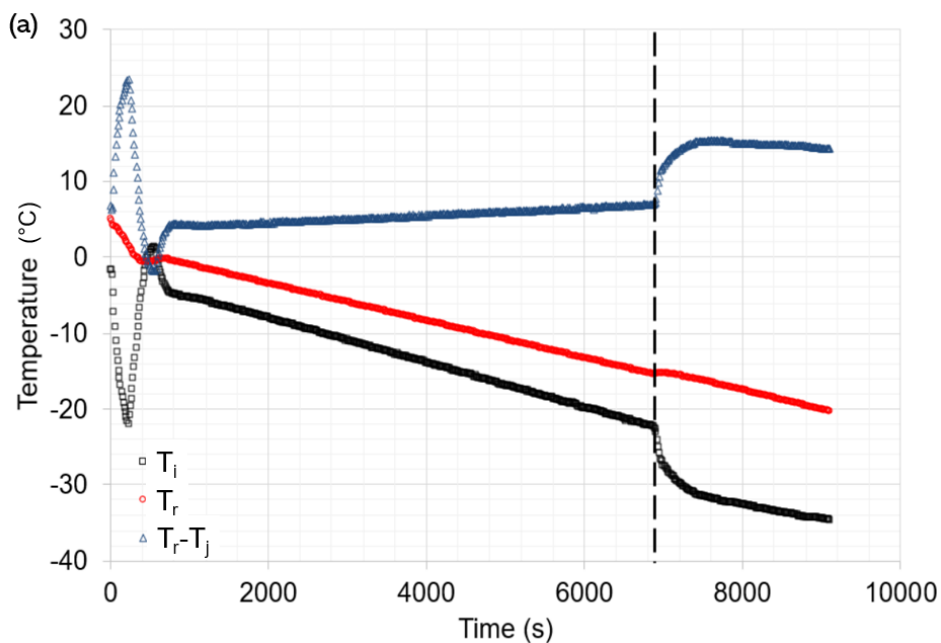
195

196 3.2 Phase diagram

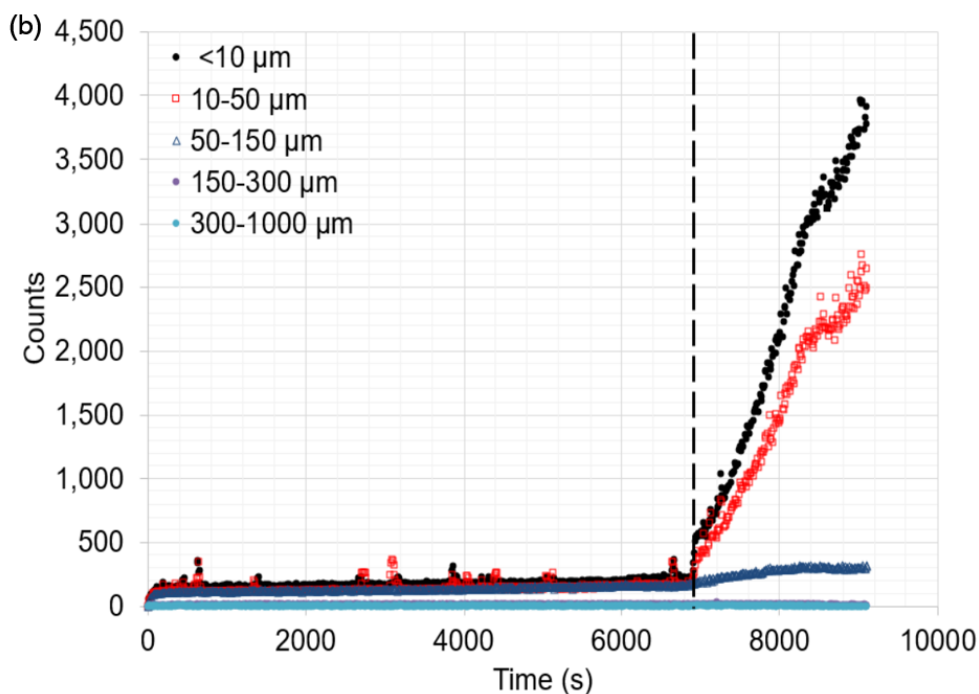
197 The phase diagram for the NaCl-H₂O system was first validated against the data generated by the
 198 Extended UNIQUAC model to verify the effectiveness and the reproducibility of the experiments.

199 The equilibrium solubility for NaCl-H₂O was first obtained by the first approach described in Section
 200 2.2, that of cooling NaCl solutions with known concentration from room temperature to -21 °C in the
 201 crystallization reactor. The formation of salt or ice crystals in the reactor could be identified from the
 202 change of either the cooling profile or the FBRM particle count. As an example, the temperature
 203 profile of the crystallization reactor and the jacket for 18.7 wt% NaCl is presented in Figure 4 (a). It can
 204 be seen that as crystallization occurs, a significant change in the temperature difference between the
 205 reactor and the jacket ($T_r - T_j$) is detected at 6800 s. This change can be attributed to the formation of
 206 ice crystals, as the additional latent heat released means that the jacket temperature must be lowered
 207 at a more rapid rate to maintain the cooling rate setpoint (0.15 K/min). This also corresponds to a
 208 sharp increase in the particle size counts at 6800 s due to the presence of ice crystals, as shown in
 209 Figure 4 (b). The reactor temperature at which the significant changes in ($T_r - T_j$) and the particle size

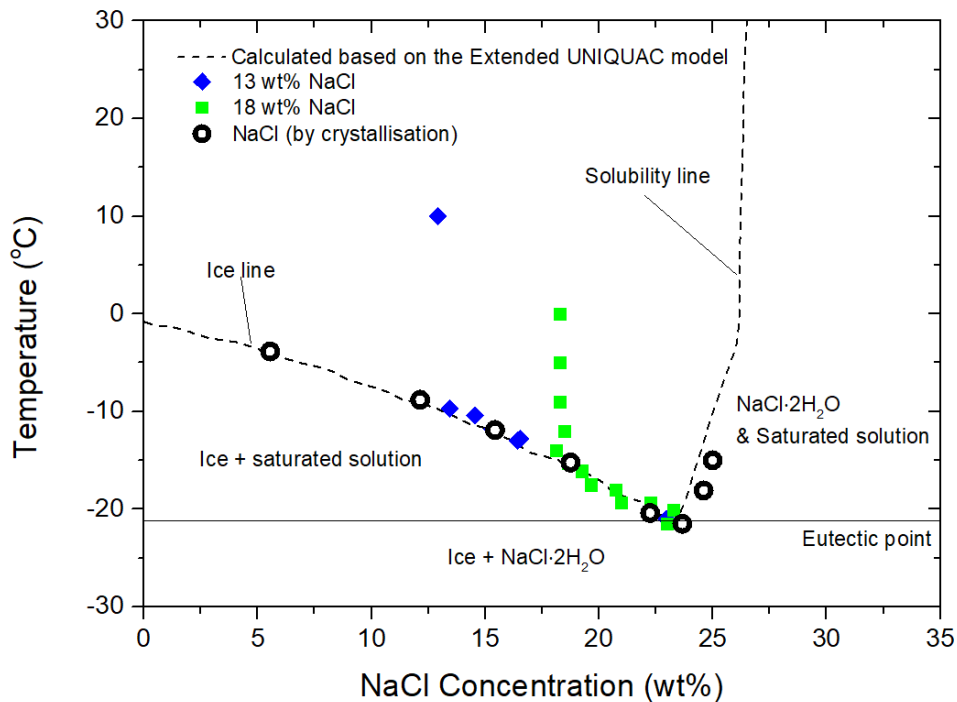
210 occur is the crystallization temperature (i.e., -15 °C for 18.7 wt% NaCl). These experiments were
 211 repeated for a range of NaCl concentrations and the corresponding crystallization temperatures were
 212 plotted against these concentrations to form the equilibrium solubility line in the phase diagram (black
 213 circles in Figure 5).



214



215
 216 Figure 4: Temperature profile of the reactor (a) and counts of particles of various size (in μm) within
 217 the reactor (b) during the crystallization of NaCl (18.7 wt%) using the OptiMax 1001 crystalliser. (T_j :
 218 Jacket Temperature; T_r : Reactor Temperature). Crystallization occurs at 6800 s on the timeline.



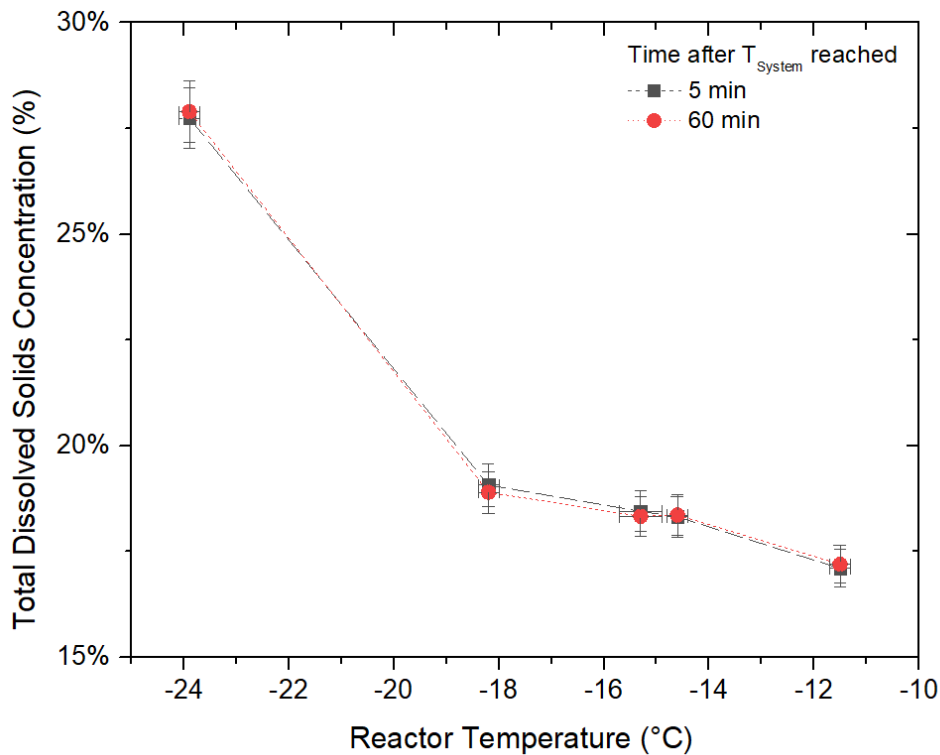
219
 220 Figure 5: Phase diagram of the NaCl-H₂O system. The crystallization temperatures of NaCl solutions of
 221 different concentrations, determined using the first approach detailed in Section 2.2 are plotted as
 222 black circles. The concentration of NaCl at different reactor temperatures, cooling from room
 223 temperature at initial concentrations of 13 wt% (blue diamonds) and 18 wt% (green squares) was
 224 estimated using the second approach detailed in Section 2.2. The phase diagram generated based on
 225 the Extended UNIQUAC model is shown as the dashed line.

226

227 A second approach to develop the phase diagram was to measure the total solids concentration in the
 228 supernatant. As shown in Figure 5, NaCl solutions of 13 wt% and 18 wt% were cooled from room
 229 temperature to -20 °C. Samples of the supernatant were collected from the middle of the reactor at
 230 different reactor temperatures, after the stirrer was paused to allow ice to float to the top of the
 231 mixture. The total dissolved solids concentration in these supernatant samples was determined and
 232 was plotted against the corresponding reactor temperature in the phase diagram. Data generated
 233 from both approaches are in agreement with the phase diagram for the NaCl-H₂O system calculated
 234 using the Extended UNIQUAC model (Figure 5), illustrating the effectiveness of either approach in
 235 developing the phase diagram using the Optimax 1001 crystalliser.

236 Salty whey from the dairy processing plant is not available as fresh samples in different concentrations.
 237 As it is a waste effluent, it is also not available in powder form for re-constitution into solutions of
 238 different concentration. Therefore, the second approach was employed as the primary mechanism to
 239 generate the phase diagram for salty whey. In order to determine the total dissolved solids
 240 concentration of the supernatant, supernatant samples of salty whey (UF permeate) at different

241 temperatures were collected within 5 minutes after a certain reactor temperature was reached. To
 242 understand if the system was in equilibrium when these samples were collected, the reactor
 243 temperature was also held at specific temperatures for 1 hour. As shown in Figure 6, within the
 244 experimental error of the total dissolved solids concentration measurements and the variation of the
 245 reactor temperature, it can be regarded that system equilibrium is achieved within the first five
 246 minutes.



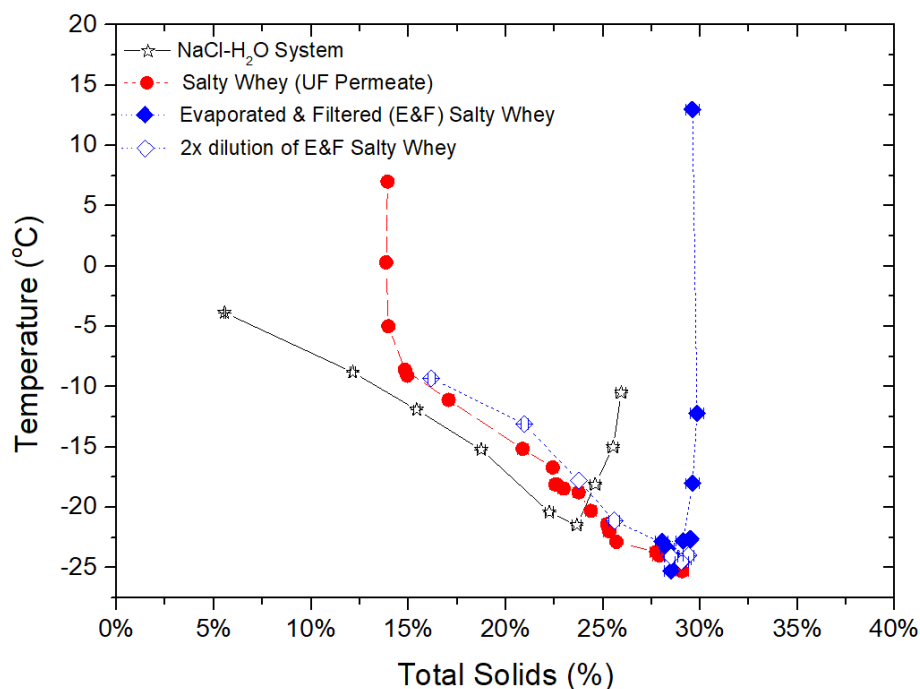
247 Figure 6: Total dissolved solids concentrations in salty whey (UF permeate) 5 min and 60 min after
 248 the reactor temperature was reached. Lines are drawn to guide the eye.
 249

250
 251 The phase diagram for salty whey was successfully constructed using this approach (Figure 7). Fresh
 252 salty whey (UF permeate) samples (~15 wt%) and the concentrated and filtered salty whey sample
 253 (~30 wt%) were cooled from room temperature to -24 °C. Total solids concentration in the
 254 supernatant for salty whey (UF permeate) increased from 14.8% ± 0.1% to 29.1% ± 0.2%, as ice crystals
 255 formed in the reactor during the cooling process. Conversely, during the cooling process of the E&F
 256 salty whey sample, salt crystallization occurred, leading to a decrease in total solids concentration in
 257 the supernatant. The cooling curve from the fresh salty whey (UF permeate) samples forms the ice
 258 line (as defined in Figure 1), while the curve obtained from the E&F salty whey samples is the solubility
 259 line (as defined in Figure 1) of salty whey.

260 It is noted that the data points for salty whey samples scatter slightly near the eutectic temperature
 261 in Figure 7, although within the measurement sensitivity of both parameters. This is probably because
 262 complete crystallization of the small quantities of calcium phosphate present in the solution can take
 263 up to 168 hours (i.e. 1 week) [20]. To validate the phase diagram, the freezing curve for the diluted
 264 E&F salty whey samples was also determined. The resulting ice line is consistent with that of the
 265 original salty whey permeate (Figure 7). This also means that natural evaporation of salty whey in solar
 266 ponds, which only concentrates the brine, would have little influence on the thermal properties in the
 267 process of eutectic freeze concentration.

268 It should be noted that the current refrigeration systems (ammonia based) in the dairy industry have
 269 the capacity to provide a cooling temperature of no lower than -20°C [7]. Hence, if spare cooling load
 270 is available within the dairy processing facilities, one of the immediate opportunities for ice/water
 271 recovery from salty whey could be considered at a temperature higher than the eutectic temperature
 272 (e.g., -15°C), where up to 40% of water (from 13%TS at $>0^{\circ}\text{C}$ to 21%TS at -15°C , see Figure 7) can be
 273 recovered as pure frozen water during a freeze concentration process.

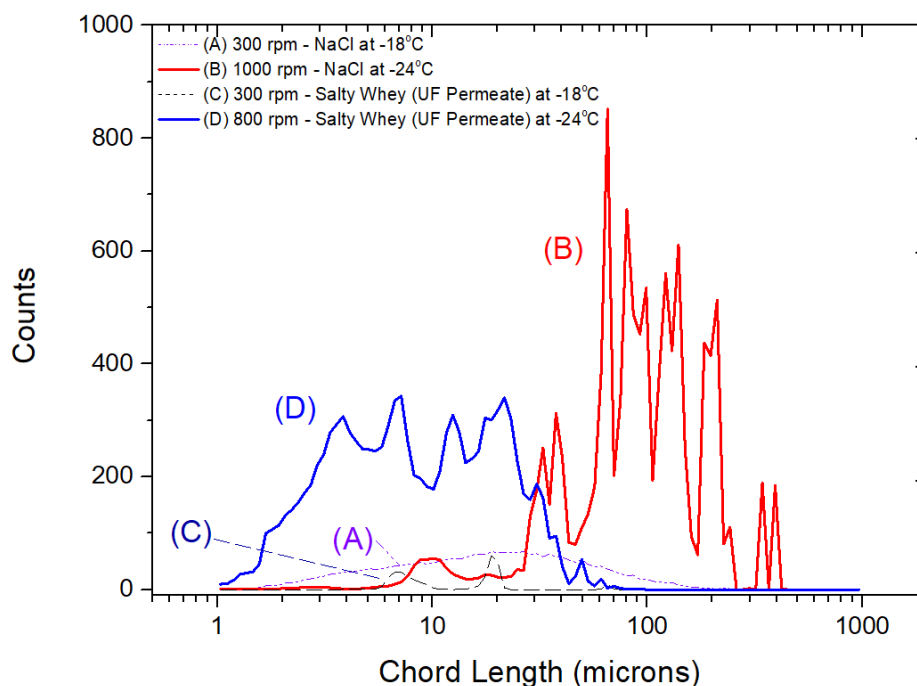
274



275
 276 Figure 7: Phase diagram of aqueous sodium chloride solution, salty whey (UF permeate), E&F salty
 277 whey and diluted E&F salty whey. Lines are drawn to guide the eye.

278 At the eutectic temperature, a complete separation of ice and salt crystals was not visually observed
 279 with the current reactor setup. This is because an 'ice jacket' (i.e., scaling) formed around the inner
 280 wall of the reactor. This scaling layer covered the limited observation window of the Optimax 1001

281 reactor and hence did not allow observation of such phenomena. Preliminary information on the size
 282 of crystals during the freezing process, was however obtained by Focused Beam Reflectance
 283 Measurement (FBRM). At different solution stirring speeds, the particle size distribution varies (Figure
 284 8). The low stirring speed (Figure 7 A and C, 300 rpm) was only used for reactor temperatures above
 285 -18°C . At -18°C , the NaCl-H₂O system has a broad distribution of crystals (Figure 7 A, median chord
 286 length: 25 microns), while the salty whey system produced a bimodal distribution with crystals of
 287 chord length 7 microns and 20 microns (Figure 7C). To allow the reactor temperature to go below $-$
 288 18°C , the stirring speed was then raised to overcome the increased heat transfer resistance caused by
 289 both the thick 'ice jacket' formed around the inner reactor wall and the increased viscosity of the
 290 solution/crystal mixture. At high stirring speeds, air bubbles were inevitably introduced in the system
 291 hence a clear particle size distribution could not be obtained. It can be seen, however, that the salty
 292 whey system produces smaller crystals (5-20 microns) than the NaCl-H₂O system (~ 100 microns). The
 293 100-micron particles in the NaCl-H₂O system were produced probably because the system
 294 temperature was allowed to go beyond its eutectic point (-24°C vs -21°C).
 295

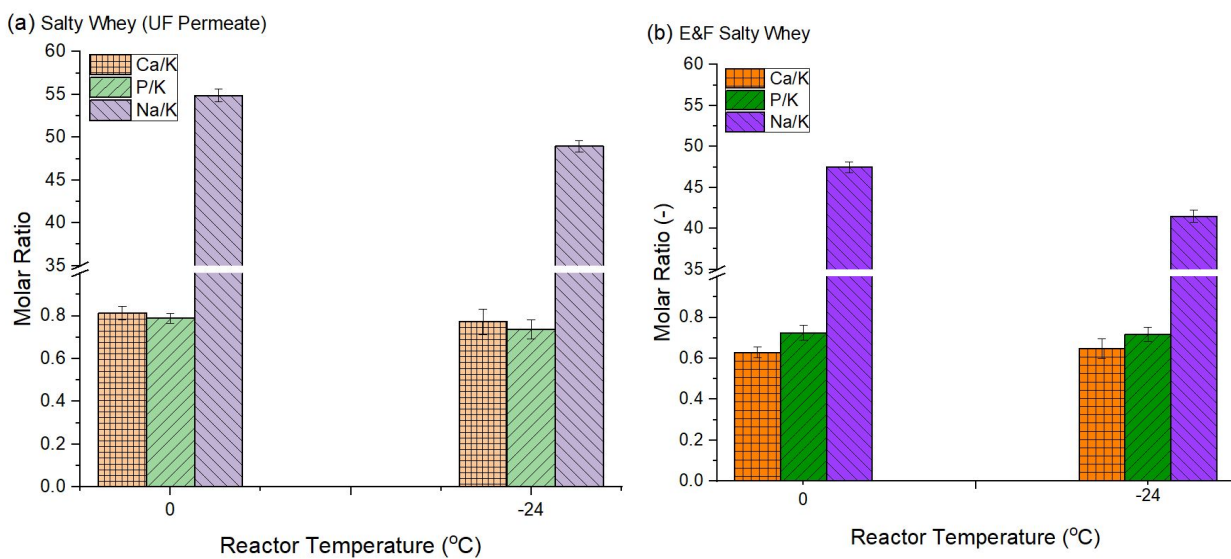


296
 297 Figure 8: Chord length distribution of crystals for NaCl solutions and salty whey at -18°C and -24°C
 298 at different stirrer speeds.

299 The composition of salt crystals created one hour after the eutectic temperature is reached was also
 300 determined indirectly from the changes in the supernatant composition. As seen in Figure 9 , for both
 301 the salty whey (UF permeate) and the E&F salty whey samples, the ratio of Na/K decreases, whereas
 302 the ratios of Ca/K and P/K remain constant at the eutectic temperature. This indicates that the crystals

303 formed at the eutectic temperature are sodium salts. This is consistent with the very slow kinetics for
 304 calcium phosphate precipitation at low temperatures, as shown in our previous study [10]. Industrial
 305 scale EFC processes separate the crystals and supernatant continuously as ice and salt crystals are
 306 formed [13, 21]. This implies that potentially pure sodium chloride salt and clean water can be
 307 simultaneously recovered from salty whey using a eutectic freeze concentration process, leaving a
 308 residual effluent that is more concentrated in calcium phosphate.

309



310 Figure 9: Molar ratio of calcium, phosphorus and sodium to potassium in the supernatant for (a)
 311 salty whey (UF permeate) and (b) evaporated and filtered salty whey samples at 0 and -24 °C.

312

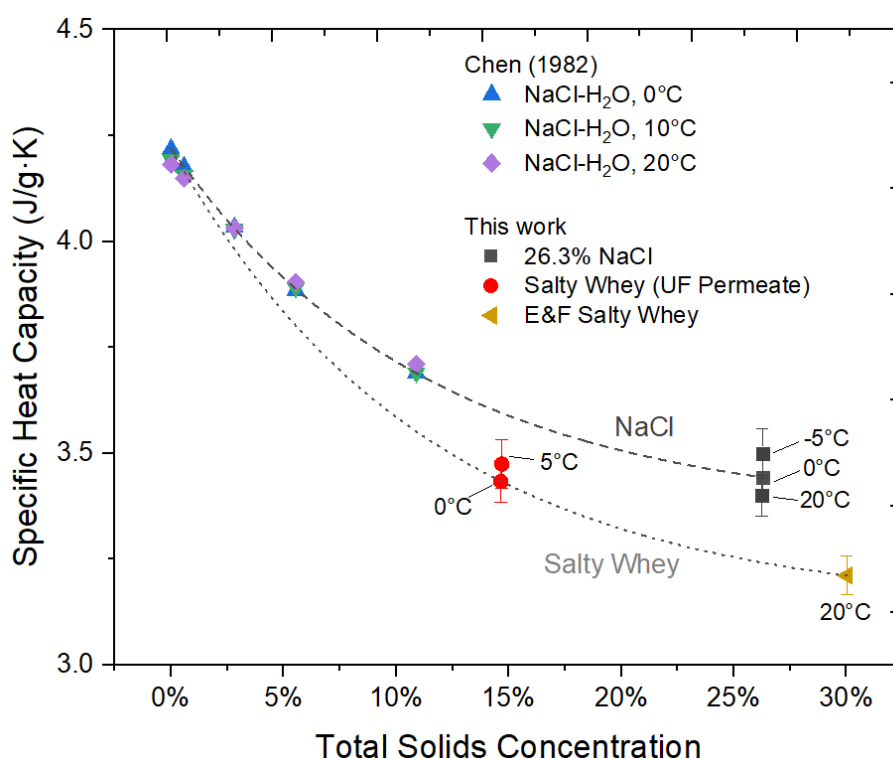
313 3.3 Energy consumption

314 The energy consumption of a continuous EFC process processing 5 wt%, 15 wt% and 30 wt% NaCl, as
 315 well as 15 wt% and 30 wt% salty whey, was estimated using the energy analysis approach reported by
 316 Van der Ham [9]. It is assumed that the process separates continuously sodium chloride salts from
 317 water, with 100% recovery and no heat loss in the system. The theoretical minimum energy
 318 requirement for an ideal EFC process was calculated as the sum of the energy requirement for cooling
 319 the feed to the eutectic temperature and the cooling required to achieve the phase changes to solid
 320 ice and salt.

321 The sensible heat required to cool the solution from 20 °C to its eutectic temperature was determined
 322 based on the specific heat capacity of sodium chloride and salty whey presented in Figure 10. The
 323 specific heat capacity of 26.3 wt% sodium chloride and salty whey (15% and 30%) was estimated using
 324 the calorimetric probe (OptiMax™ HFCal). Both literature data and the measured values show very

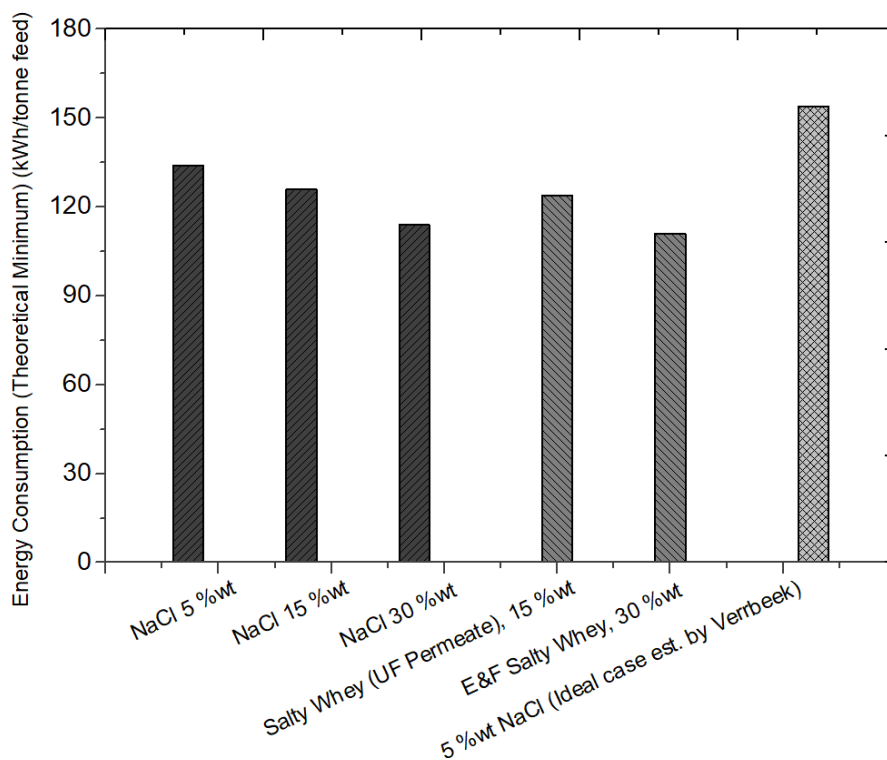
325 small variations in the heat capacity with respect to temperature. The cooling requirement for ice and
 326 salt formation was estimated based on the enthalpy of crystallization/formation of ice (6.012 kJ/mol)
 327 and sodium chloride dihydrate (6.8 kJ/mol, averaged from values reported in Drebushchak and
 328 Ogienko [22], Verbeek [23] and Swenne [24]).

329 As shown in Figure 11, the minimum energy required is similar between pure NaCl solutions and salty
 330 whey with the same total solids concentrations, since salty whey contains primarily NaCl. Increasing
 331 the salty whey concentration from 15wt% to 30wt% reduces the energy demand by 11% (from 125
 332 kWh/tonne feed to 111 kWh/tonne feed). This is due to the reduced latent heat required to generate
 333 ice crystals as there is less water present, as well as the lower specific heat capacity of solutions at
 334 higher concentrations (Figure 10). The estimate from the ideal case presented in Verrbeek [23] for 5
 335 wt% solution is slightly higher, because Verrbeek took into consideration the washing of ice and salt
 336 downstream in a wash column and a belt filter. For optimized thermal brine concentrator-crystalliser
 337 systems, >80 kWh/m³ feed (<65,000 ppm, equiv. to ~6 wt%) is required [25] which is a little less than
 338 that presented in Figure 11. It should be noted that EFC is still an emerging technology and
 339 improvement in process design and energy integration could result in enhanced energy efficiency in
 340 the future.



341 Figure 10: Specific heat capacity of NaCl solutions of different concentrations reported in the literature
 342 by Chen [26] and that of 26.3 wt% NaCl and salty whey samples measured in this work using the
 343 calorimetric probe (OptiMax™ HFCal). Lines are drawn to guide the eye.
 344

345



347
 348 Figure 11: Theoretical minimum energy required for processing one tonne of different brine solutions
 349 by EFC with 100% water and NaCl recovery. Data for the 5 wt% NaCl ideal case is reported by Verbeek
 350 [23].

351

352 4. CONCLUSIONS

353

354 Fresh salty whey samples collected from a dairy processing facility in Victoria, Australia were used to
 355 construct the solid-liquid phase diagram of salty whey under equilibrium conditions. The eutectic point
 356 of salty whey was found to be at -24°C , lower than that of NaCl solutions (-21°C). The temperature-
 357 total solids concentration relationship is similar, however, to that attained for these aqueous sodium
 358 chloride solutions. Pure NaCl salts and ice were formed within 5 minutes after the eutectic
 359 temperature was reached, as determined by monitoring the changes of cation composition in the
 360 supernatant at the eutectic temperature. The lower eutectic temperature makes it difficult for
 361 eutectic freeze crystallization to be operated with ammonia-based refrigeration systems and hence
 362 simple freeze crystallization at -15°C may be more attractive. The energy consumption of the eutectic
 363 freeze crystallization process was estimated to be in the range of 111 to 125 kWh/tonne for salty whey
 364 samples (15 wt% and 30 wt%). This energy demand could potentially be reduced through energy
 365 integration with onsite refrigeration processes. The energy requirement for cooling the dairy brine
 366 solutions to their eutectic point is in the same order of magnitude as that for using conventional

367 thermal brine concentrators and crystallisers (80 kWh per tonne feed).

368

369 **ACKNOWLEDGEMENT**

370

371 The Australian Research Council's Industrial Transformation Research Program (ITRP) funding scheme
372 (project number IH120100005). The ARC Dairy Innovation Hub is a collaboration between The
373 University of Melbourne, The University of Queensland and Dairy Innovation Australia Ltd.

374

375 **REFERENCES**

376

- 377 [1] G.Q. Chen, S.L. Gras, S.E. Kentish, Separation Technologies for Salty Wastewater Reduction in the
378 Dairy Industry, *Separation & Purification Reviews*, (2018) 1-29.
- 379 [2] G.Q. Chen, S. Talebi, S.L. Gras, M. Weeks, S.E. Kentish, A review of salty waste stream
380 management in the Australian dairy industry, *J. Environ. Manage.*, 224 (2018) 406-413.
- 381 [3] P. Bharmoria, H. Gupta, V.P. Mohandas, P.K. Ghosh, A. Kumar, Temperature Invariance of NaCl
382 Solubility in Water: Inferences from Salt-Water Cluster Behavior of NaCl, KCl, and NH₄Cl, *The Journal*
383 *of Physical Chemistry B*, 116 (2012) 11712-11719.
- 384 [4] D.R. Heldman, D.B. Lund, C. Sabliov, *Handbook of Food Engineering*, CRC Press, 2006.
- 385 [5] R.W. Hartel, L.A. Espinel, Freeze concentration of skim milk, *J. Food Eng.*, 20 (1993) 101-120.
- 386 [6] M.V. Rane, D.B. Uphade, Energy Efficient Jaggery Making Using Freeze Pre-concentration of
387 Sugarcane Juice, *Energy Procedia*, 90 (2016) 370-381.
- 388 [7] P. Williams, M. Ahmad, B. Connolly, Freeze desalination: An assessment of an ice maker machine
389 for desalting brines, *Desalination*, 308 (2013) 219-224.
- 390 [8] P.M. Williams, M. Ahmad, B.S. Connolly, D.L. Oatley-Radcliffe, Technology for freeze
391 concentration in the desalination industry, *Desalination*, 356 (2015) 314-327.
- 392 [9] F. van der Ham, G.J. Witkamp, J. de Graauw, G.M. van Rosmalen, Eutectic freeze crystallization:
393 Application to process streams and waste water purification, *Chemical Engineering and Processing:*
394 *Process Intensification*, 37 (1998) 207-213.
- 395 [10] S.T. Reddy, A.E. Lewis, G.J. Witkamp, H.J.M. Kramer, J. van Spronsen, Recovery of
396 Na₂SO₄·10H₂O from a reverse osmosis retentate by eutectic freeze crystallization technology,
397 *Chem. Eng. Res. Des.*, 88 (2010) 1153-1157.
- 398 [11] R.J.C. Vaessen, B.J.H. Janse, M.M. Seckler, G.J. Witkamp, Evaluation of the Performance of a
399 Newly Developed Eutectic Freeze Crystallizer: Scraped Cooled Wall Crystallizer, *Chem. Eng. Res. Des.*,
400 81 (2003) 1363-1372.
- 401 [12] J. Van Spronsen, M.R. Pascual, F.E. Genceli, D.O. Trambitas, H. Evers, G.J. Witkamp, Eutectic
402 freeze crystallization from the ternary Na₂CO₃-NaHCO₃-H₂O system: A novel scraped wall
403 crystallizer for the recovery of soda from an industrial aqueous stream, *Chem. Eng. Res. Des.*, 88
404 (2010) 1259-1263.
- 405 [13] M.J. Fernández-Torres, F. Ruiz-Beviá, M. Rodríguez-Pascual, H. von Blottnitz, Teaching a new
406 technology, eutectic freeze crystallization, by means of a solved problem, *Education for Chemical*
407 *Engineers*, 7 (2012) e163-e168.
- 408 [14] M.J. Fernández-Torres, D.G. Randall, R. Melamu, H. von Blottnitz, A comparative life cycle
409 assessment of eutectic freeze crystallization and evaporative crystallization for the treatment of
410 saline wastewater, *Desalination*, 306 (2012) 17-23.
- 411 [15] D.G. Randall, J. Nathoo, A.E. Lewis, A case study for treating a reverse osmosis brine using
412 Eutectic Freeze Crystallization—Approaching a zero waste process, *Desalination*, 266 (2011) 256-
413 262.

- 414 [16] K. Kezia, J. Lee, M. Weeks, S. Kentish, Direct contact membrane distillation for the concentration
415 of saline dairy effluent, *Water Res.*, 81 (2015) 167-177.
- 416 [17] A. Ruf, J. Worlitschek, M. Mazzotti, Modeling and Experimental Analysis of PSD Measurements
417 through FBRM, *Particle & Particle Systems Characterization*, 17 (2000) 167-179.
- 418 [18] A. Hvidt, K. Borch, NaCl-H₂O Systems at temperatures below 273 k, studied by differential
419 scanning calorimetry, *Thermochim. Acta*, 175 (1991) 53-58.
- 420 [19] P.H. Rasmussen, B. Jørgensen, J. Nielsen, Aqueous solutions of proline and NaCl studied by
421 differential scanning calorimetry at subzero temperatures, *Thermochim. Acta*, 303 (1997) 23-30.
- 422 [20] K. Kezia, J. Lee, B. Zisu, G.Q. Chen, S.L. Gras, S.E. Kentish, Solubility of Calcium Phosphate in
423 Concentrated Dairy Effluent Brines, *Journal of Agricultural and Food Chemistry*, 65 (2017) 4027-
424 4034.
- 425 [21] F.E. Genceli, Scaling-Up Eutectic Freeze Crystallization, in: *Mechanical Maritime and Materials*
426 *Engineering*, Technische Universiteit Delft, 2008.
- 427 [22] V.A. Drebuschak, A.G. Ogienko, Calorimetric measurements of sodium chloride dihydrate
428 (hydrohalite), *J. Therm. Anal. Calorim.*, (2019).
- 429 [23] B. Verbeek, Eutectic Freeze Crystallization on Sodium Chloride, Analysis of a full experimental
430 cycle, in: *Faculty of Process Equipment*, Delft University of Technology, Netherlands, 2011.
- 431 [24] D.A. Swenne, The eutectic crystallization of NaCl.2H₂O and ice, in: *Department of Chemical*
432 *Engineering and Chemistry*, Technische Hogeschool Eindhoven, 1983.
- 433 [25] M. Mickley, Survey of high-recovery and zero liquid discharge technologies for water utilities, in,
434 *Water Reuse Foundation*, 2008.
- 435 [26] C.T.A. Chen, Specific heat capacities of aqueous sodium chloride solutions at high pressures,
436 *Journal of Chemical & Engineering Data*, 27 (1982) 356-358.

437

438

439 **Tables**

440

441 Table 1: General characteristics and composition of salty whey (UF permeate), evaporated and
442 filtered salty whey (E&F Salty Whey) and diluted E&F salty whey (Dil-E&F Salty Whey).

443

444

445

446 Figure Captions

447

448 Figure 1: A typical phase diagram for aqueous salt solutions showing the Eutectic point [13].
449 (Copyright 2012, with permission from Elsevier.)

450 Figure 2: The schematic of OptiMax 1001 crystalliser equipped with temperature, heat flow and
451 FBRM sensors (left); and a photo of the crystalliser without showing the water bath and computers
452 (b).

453 Figure 3: DSC thermograms (heat flow vs. temperature) measured during cooling (I and II) from 30°C
454 to -80 °C and subsequent heating (III and IV) for (a) 13.8% NaCl in water, (b) salty whey (UF
455 permeate) and (c) evaporated & filtered salty whey. The scanning rate was 3°C/min for both cooling
456 and heating steps. The eutectic temperatures were determined to be -20.9 ± 0.2 °C, -23.6 ± 0.3 °C,
457 and -24.2 ± 0.3 °C for 13.8% NaCl in water, salty whey (UF permeate) and evaporated & filtered salty
458 whey, respectively.

459 Figure 4: Temperature profile of the reactor (a) and counts of particles of various size (in μm) within
460 the reactor (b) during the crystallization of NaCl (18.7 wt%) using the OptiMax 1001 crystalliser. (T_j :
461 Jacket Temperature; T_r : Reactor Temperature). Crystallization occurs at 6800 s on the timeline.

462 Figure 5: Phase diagram of the NaCl-H₂O system. The crystallization temperatures of NaCl solutions
463 of different concentrations, determined using the first approach detailed in Section 2.2 are plotted
464 as black circles. The concentration of NaCl at different reactor temperatures, cooling from room
465 temperature at initial concentrations of 13 wt% (blue diamonds) and 18 wt% (green squares) was
466 estimated using the second approach detailed in Section 2.2. The phase diagram generated based on
467 the Extended UNIQUAC model is shown as the dash line.

468 Figure 6: Total dissolved solids concentrations in salty whey (UF permeate) 5 min and 60 min after
469 the reactor temperature was reached. Lines are drawn to guide the eye.

470 Figure 7: Phase diagram of aqueous sodium chloride solution, salty whey (UF permeate), E&F salty
471 whey and diluted E&F salty whey. Lines are drawn to guide the eye.

472 Figure 8: Chord length distribution of crystals for NaCl solutions and salty whey at -18°C and -24°C
473 at different stirrer speeds.

474 Figure 9: Molar ratio of calcium, phosphorus and sodium to potassium in the supernatant for (a)
475 salty whey (UF permeate) and (b) evaporated and filtered salty whey samples at 0 and -24 °C.

476 Figure 10: Specific heat capacity of NaCl solutions of different concentrations reported in the
477 literature by Chen [26] and that of 26.3 wt% NaCl and salty whey samples measured in this work
478 using the calorimetric probe (OptiMax™ HFCal). Lines are drawn to guide the eye.

479 Figure 11: Theoretical minimum energy required for processing one tonne of different brine
480 solutions by EFC with 100% water and NaCl recovery. Data for the 5 wt% NaCl ideal case is reported
481 by Verbeek [23].

482

483

484

485